CHAPTER 3

To study the expression and sub-cellular localization of MeCP2 in glial cells

3.1 Introduction

MeCP2 is an essential epigenetic modulator in the mammalian CNS which not only function as a transcriptional repressor but also as an activator via binding to methylated CpGs in the promoters and nearby regions of target genes (Chahrour et al., 2008). MeCP2 undergoes various post translational modifications (PTMs), including phosphorylation, acetylation, ubiquitination and sumoylation, whose functional roles remain largely unexplored (Bellini et al 2014.; Li et al., 2014).

MeCP2 are phosphorylated at multiple sites, of which the well-documented MeCP2 phosphorylation sites are S80 and S421; phosphorylation of these sites modulates the transcription of their target genes in opposite manners leading to gene silencing or activation respectively (Chao and Zoghbi, 2009; Rutlin and Nelson, 2011; Tao et al., 2009; Zhou et al., 2006). Activity-dependent phosphorylation of MeCP2 at serine 421 leads to separation of MeCP2 from the promoter (Zhou et al., 2006) whereas, resting condition influences phosphorylation of serine S80, which promotes the binding of MeCP2 to the promoters of target genes for repression (Tao et al., 2009). These findings illustrate the diversity and complexity of site specific MeCP2 phosphorylation (Cheng et al., 2014).

Differential phosphorylation of MeCP2 is a key mechanism by which the methyl binding protein modulates its affinity for its partners, gene expression and cellular adaptations to stimuli and neuronal plasticity. Alterations in neuronal morphology, circuit formation, and mouse behavioral phenotypes were found in phospho-defective MeCP2 knock-in mice at S80 and S421 sites of MeCP2 (Bellini et al., 2014). Previously, RTT was attributed solely to neuronal dysfunction. However, recent studies have shown that mutation in glial MeCP2 mainly oligodendrocytes, astrocytes and microglia, are an integral part of manifestation of RTT, affecting neuronal structure and function (Ballas et al., 2009; Derecki et al., 2012; Lioy et al., 2011; Maezawa and Jin, 2010; Nguyen et al., 2013; Vora et al.,2010).

OLGs are glial cells that produce and maintain myelin, which is essential for saltatory conduction of action potentials in the neurons of central nervous system (CNS). OLGs

originate as progenitors and after receiving synaptic inputs from neurons they myelinate axons by producing a greater number of sheaths (Almeida et al., 2011; Bergles et al., 2010). Apart from playing a critical role in propagation of neuronal signaling, they are also crucial for axonal support (Baumann and Pham-Dinh, 2001; Saab et al., 2013). One study revealed that brain magnetic resonance study in Mecp2-/y mice detected a significant reduction in the thickness of the corpus callosum which shows that white matter is affected in Rett syndrome (Saywell et al., 2006). Furthermore, it has been reported recently that myelin gene expression is altered in MeCP2-null mice (Nguyen et al., 2013; Sharma et al., 2015; Vora et al.).

On the other hand, astrocytes maintain and regulate the level of fluid, pH, ions and neurotransmitters at synapse, provide nutrients and structural support around synapses, and contribute to the integrity of the blood brain barrier (BBB) (Brown and Ransom, 2007). Evidence has further shown that, like neurons, astrocytes of MeCP2-null mice also exhibit RTT like symptoms (Nguyen et al., 2013). Astrocytes derived from MeCP2 null mice model of RTT show alterations of gene expression and glutamate (Okabe et al., 2012). Moreover, the MeCP2 deficient astrocytes are abnormal and can progressively spread MeCP2 deficiency via gap junction communication of novel non-cell autonomous mechanism (Maezawa et al., 2009). Importantly, re-expression of MeCP2 specifically in astrocytes, RTT mice significantly improves motor activities and behaviors, as well as prolongs lifespan to nearly normal (Derecki et al., 2012; Lioy et al., 2011).

In spite of the important role of glia in the brain function, the critical question of how oligodendrocytes and astrocytes contribute to RTT neuropathology has not been addressed at large. Most studies have reported pMeCP2s exclusively in neurons (Li et al., 2011; Tao et al., 2009), but there is hardly any information available so far on these PTMs and their regulation during brain development; particularly in glia, except for the recent observations of p292MeCP2, pS80MeCP2 and pS421MeCP2 in astrocytes (Liu et al., 2015; Liu et al., 2017). Moreover, it was demonstrated that MeCP2 and diverse pMeCP2s have distinct features of spatio-temporal expression in the rat brain, and that the precise levels ofMeCP2 in the postnatal period are vital to cerebellar neural cell development (Liu et al., 2017).

Therefore, the focus of the present *invitro* study was to identify the expression and distribution patterns of pS80 MeCP2, pS421 MeCP2, and total MeCP2 in the glial cells of CNS particularly OLGs and astrocytes. As to intracellular localization, MeCP2 occurs predominantly in the nucleus, but it can be also expressed in the cytoplasm and postsynaptic compartment at a relatively low level (Miyake and Nagai, 2007). The precise levels of MeCP2 are vital for brain development. Its abnormal expression causes Rett syndrome (RTT), a genetic neurological disorder (Amir et al., 1999). Hence, this study also investigated the intracellular localization of pMeCP2s in the rat glial cells of CNS to assist further understanding of MeCP2 function.

3.2 Plan of work

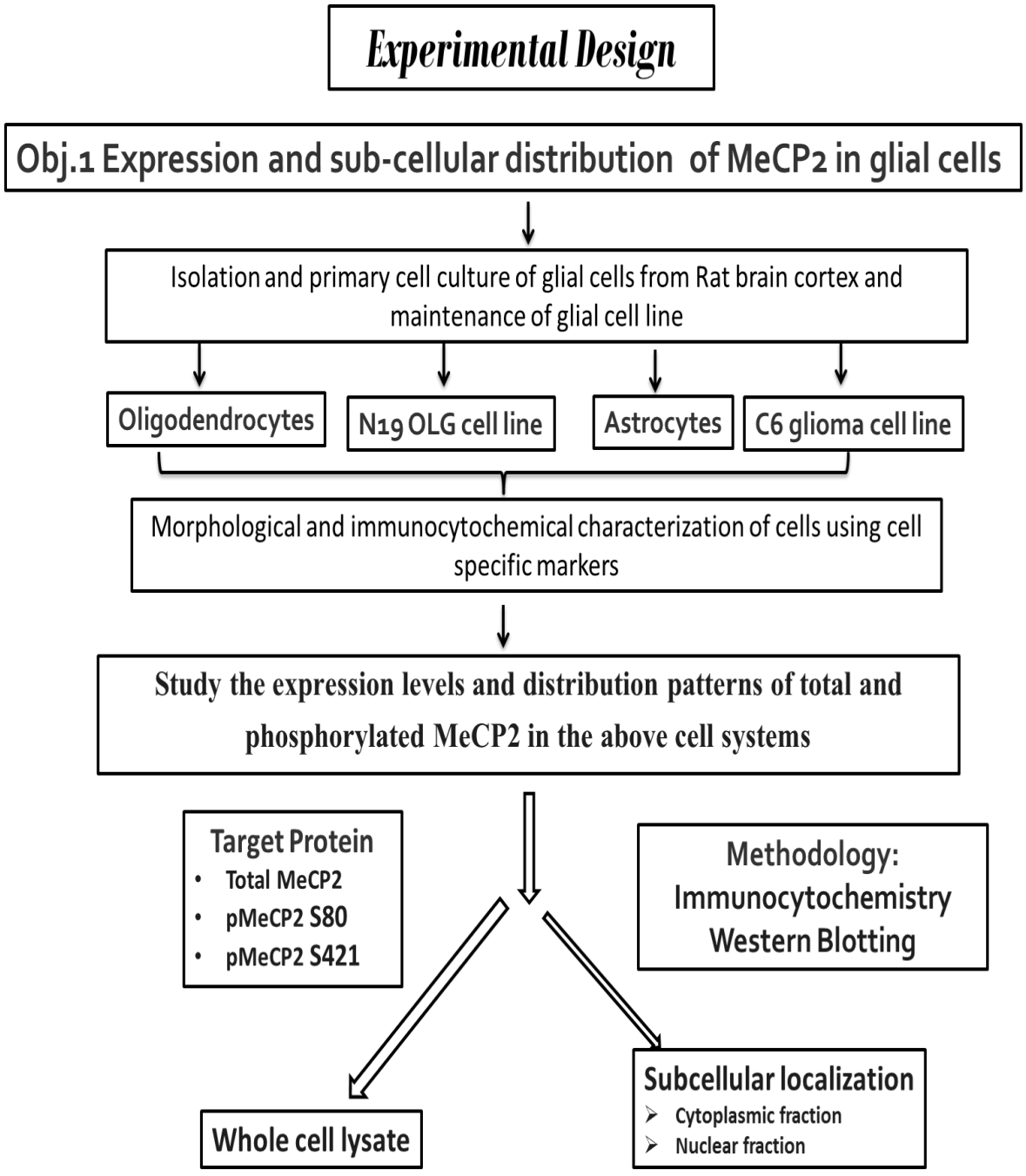

3.3 Results

3.3.1 Glial cells isolation and characterization

In the present study, the glial cells were isolated from the cortical region of rat brain of P0 day pups following standard protocol (refer Materials and Methods in Chapter 2). Briefly, oligodendrocytes are separated from the bed of astrocytes by overnight shaking. Oligodendrocytes were allowed to differentiate in Sato medium without PDGF-A. Morphological changes were observed at each stage of oligodendrocyte development from oligodendrocyte precursor cells (OPCs) to immature OLGs and then finally mature OLGs [Fig. 3.1 (A) –a, b & c].Then the oligodendrocytecells were fixed on 4thday and 12thday and subjected to immunocytochemical characterization by stages pecific markers. Representative immunostaining images showing 4thday Immature OLGs with anti-O4 (red) and 12thday mature OLGs with anti-MBP (red). The nucleus was stained with DAPI (blue). Scale bar=20µm [Fig.3.1 (B) - d & e]. The cortical astrocytes were also characterized using cell specific marker. Under basal conditions, astrocytes presented a polygonal to fusiform and flat morphology [Fig. 3.1 (A)–e]. Furthermore, after immunostaining the cells were positive for Glial fibrillary acidic protein- GFAP (green) which is considered as the one of the marker for astrocytic cells. The nucleus was stained with DAPI (blue). Scale bar=20µm[Fig. 3.1 (B) - c].

Additionally, to study the oligodendrocytes, mouse oligodendroglial cell line N19 was also employed. This cell line was a kind gift from Dr.Pablo Paez (Department of Pharmacology and Toxicology, Hunter James Kelly Research Institute, School of Medicine and Biomedical Sciences, SUNY, University at Buffalo, NYS Center of Excellence, 701 Ellicott St., Buffalo, New York, USA). These cells were conditionally immortalized OLGs. These cells have a similar morphology like OLGs [Fig 3.1 (A)-d]. Phenotypic characterization was done using markers. Immunostaining images showing immature N19 OLGs with anti-PDGFRα (green) and mature N19 OLGs with anti-MBP (green). The nucleus was stained with DAPI (blue). Scale bar = 20 µm [Fig 3.1 (B)- a & b]. We also used C6 glioma cell line which is widely used as an astrocyte-like cell line.

This cell line shows astrocytic like property and also expresses the GFAP which is the marker for astrocytes. [Fig 3.1 (A)-f]

3.3.2 MeCP2 phosporylation at S80 is increased during oligodendrocyte differentiation

First, we attempted to assess the MeCP2 expression in primary oligodendrocytes by immunocytochemistry and western blotting. MeCP2 expression was confirmed at both the stages of oligodendrocytes development which includes immature OLGs and mature OLGs by immunostaining [Fig 3.2 (A)]. Scale bar=50µm. Further, the MeCP2 protein expression levels were assessed by immunoblotting in immature and mature OLGs and found significant up-regulation *(***P<0.001)* in mature OLGs [Fig 3.2 (C & D)].

To investigate the expression of phospho-MeCP2s mainly, pS80MeCP2 and pS421MeCP2 in oligodendrocytes, we used MeCP2 phospho-site-specific antibodies which are available commercially (see Materials and Methods – Chapter 2). The specificity of these antibodies against pS80MeCP2, pS421MeCP2was validated by the treatment of alkaline phosphatase (PPTase) to the protein extracts from rat brain cortex. The pS80MeCP2 and pS421MeCP2 band were abolished upon phosphatase treatment (Fig 3.4-A). We used lysate of brain cortex as control to confirm the specificity of the antibodies. There was no expression of pS421MeCP2 in oligodendrocytes [Fig 3.4 (B & C)]. However, there was significant up-regulation (***P<0.01)* of pS80MeCP2 protein expression in the mature OLGs compared to the immature ones [Fig 3.2 (C & E)].

Next, to confirm the intracellular localization of pS80MeCP2, we performed immunofluorescent double staining with DAPI in the immature and mature OLGs and found that pS80 MeCP2 was completely co-localized with DAPI [Fig 3.2 (B)] scale bar=50µm. Cytoplasmic and nuclear fractions were isolated from immature and mature OLGs using NEPER Kit (Refer Materials & Methods in Chapter 2). The nuclear and cytoplasmic fraction isolation was optimized using astrocytes and the purity of the fractions was checked using GAPDH and H3 expressions which are the cytoplasmic and nuclear markers respectively (Fig 3.6). Western blot analysis of the MeCP2 and pS80MeCP2 was detected only in the nuclear fraction but not in the cytosolic fraction of

immature and mature OLGs [Fig 3.7 (A & B)]. These results demonstrated that the intracellular localizations of MeCP2 and the pMeCP2s were identical.

All the above experiments were performed in N19 cell line to validate the expression and distribution patterns of MeCP2 and phosphoMeCP2s. We first checked the expression of pS80MeCP2 and pS421MeCP2 in N19 OLGs. To confirm the expression of these proteins we used brain lysate as a positive control [Fig 3.3 (A & B)]. We did not get the expression of pS421MeCP2 in N19 cell line [Fig 3.4 (B & C)]. Immunoblotting was performed to study the expression levels of pS80MeCP2 in N19 OLGs.pS80MeCP2 was significantly found to be higher (*$**P<0.01$*) in mature N19 OLGs compared to immature N19 OLGs [Fig 3.5 (A & B)]. Further, to study the localization of pS80MeCP2 we used immunocytochemistry and the confocal microscopy imaging showed the nuclear localization of the pS80MeCP2 in N19 OLGs [Fig 3.3 (C)] Scale bar=50µm.

3.3.3 Differential distribution of MeCP2 phosphorylation in astrocytes

We checked the MeCP2 and phosphor MeCP2s expression in primary astrocytes by immunocytochemistry [Fig 3.8 (A, B & C)]. Nuclear and cytoplasmic fractions were separated and MeCP2 and phosphoMeCP2s expression was assessed using western blot analysis [Fig 3.9 (A & B)]. Thus, the data indicates that MeCP2 and pS80 MeCP2 were predominant in the nuclear fraction, while pS421MeCP2 was expressed in the cytoplasm [Fig 3.9 (A & B)]. Taken together, these results demonstrated that the expression patterns of MeCP2 and the pMeCP2s are distinct in the cortical astrocytes. Next, we also checked the expression of MeCP2 and phosphoMeCP2s (S80 & S421) in C6 glioma cell line. Nuclear and cytoplasmic fractions were separated and MeCP2 and phosphoMeCP2s expression was analyzed following western blotting [Fig 3.10 (A & B)]. Consistent with the data of primary astrocytes we got similar data in C6 glioma cell line. The data indicated that MeCP2 and pS80 MeCP2 were predominant in the nuclear fraction, while pS421 MeCP2 was expressed in the cytoplasm [Fig 3.10 (A & B)]. Further, we also assessed and confirmed the MeCP2 and phosphoMeCP2s localization by immunofluorescence C6 glioma cell line [Fig 3.11 (A, B & C)]. These results in C6

glioma cell line demonstrated that the expression patterns of MeCP2 and the pMeCP2s are in accordance with that of primary cortical astrocytes.

3.4 Discussion

MeCP2 is a global transcriptional regulator that binds at either methylated or non-methylated part of the genome. Aberrant expression and dysfunction of MeCP2 is known to cause the neurological disorder RTT (Hagberg et al., 1983). Studies have shown that both MeCP2-null mice and MeCP2 transgenic mice possess the characteristics of RTT (Collins et al., 2004; Guy et al., 2001). Moreover, the MeCP2 deficiency results in global changes in the neuronal chromatin structure (Skene et al., 2010) indicating that the accurate level of MeCP2 is vital to normal brain development. Moreover, MeCP2 has been found to be localized outside the nucleus i.e within the cytoplasm and post-synaptic compartment in neurons (Miyake and Nagai, 2007; Mnatzakanian et al., 2004). These findings have demonstrated that that the phosphorylation of MeCP2 controls the transcriptional function of MeCP2 by regulating its intracellular localization. Accumulated evidences suggest that MeCP2 could be phosphorylated at multiple sites, of which the well-documented MeCP2 phosphorylation sites are S421 and S80; phosphorylation of which modulates the transcription in opposite manners leading to gene silencing or activation (Chao and Zoghbi, 2009; Rutlin and Nelson, 2011; Tao et al., 2009; Zhou et al., 2006). Strikingly, other studies have further shown that the transcriptional roles of pS421MeCP2 and pS80MeCP2 vary according to their specific target genes, and that pS421MeCP2 can even bind across the genome without selectivity (Cohen et al., 2011). Animal model studies have further shown that even the loss of a specific phosphorylation site of MeCP2 (S80, S421) disturbs normal maturation of the mammalian brain (Tao et al., 2009). Earlier, reports have also shown that, unlike S421 phosphorylation, S80 phosphorylation not only occurs in neuronal cells but also seen in non-neuronal cells such as Hela cells and human fibroblasts (Bracaglia et al., 2009; Tao et al., 2009). Tao et al (2009) found that S80 phosphorylation is the highly conserved phosphorylation site of MeCP2. Notably, pS80MeCP2 and pS421MeCP2 can interact

with distinct co-factors to initiate disparate transcriptional pathways (Gonzales et al., 2012), indicating that the dynamic balance between phosphorylation and dephosphorylation is crucial for MeCP2 function. However, there are hardly any reports on the precise levels and expression patterns of MeCP2 and phosphorylated MeCP2 in glial cells of CNS. Earlier studies carried out prior to 2009, were focused on MeCP2 function in neurons; however the effects in non-neuronal cells in the brain were generally overlooked. Though the Magnetic resonance imaging (MRI) and Magnetic resonance spectroscopy (MRS) data from some of the studies showed that not only neuronal but also glial metabolism was affected in RTT mouse brain (Saywell et al., 2006; Viola et al., 2007).

In this study, we investigated the expression and distribution patterns of MeCP2, pS80MeCP2 and pS421MeCP2 in the glial cells of CNS mainly oligodendrocyte and astrocytes. Our data showed phosphorylated MeCP2 (S80 & S421) expression in oligodendrocytes both in primary cells as well as in the immortalized cell line of oligodendrocytes (Fig 3.2, Fig 3.3 & Fig 3.5). The study revealed that the expression of MeCP2 increased with oligodendrocyte maturation (Fig 3.2 & Fig 3.5). Consistently, it was also observed that an increase in the pS80MeCP2 level occurs when OLGs are mature. This may implicate that the precise level of MeCP2 as well as pS80MeCP2is necessary for oligoendrocyte differentiation and maturation. In primary oligodendrocytes and N19 cell line of oligodendrocytes, it was found that MeCP2 and pS80MeCP2 were concentrated in the nucleus (Fig 3.7). Further, the pS421 expression in immature andmature OLGs was analyzed. Western blotting was used to check the pS421MeCP2 expression but neither immature nor mature OLGs showed presence of clear band of pS421 MeCP2. Brain cortex was used as a positive control in which we could get a clear band of pS421 MeCP2 expression (Fig.3.4). This may be due to the cell type specific expression of phosphoMeCP2s. The study revealed that there is an increase in the expression of MeCP2 and pS80 MeCP2 during the OLG development but pS421 MeCP2 was not detected throughout the OLG development. However, there was no change in the localization pattern of MeCP2 and pS80 MeCP2. Both MeCP2 and pS80 MeCP2 were localized in nucleus. The results are in accordance with already published data in

neurons where it has been observed that MeCP2 increase during the postnatal period and have a major role in maturation (Balmer et al., 2003). Moreover a recent study Nguyen et al., 2013**,** have reported that MeCP2 deficiency in oligodendrocytes results in down-regulation of myelin gene expression and impacts myelination which strongly suggests the role of MeCP2 in maturation of oligodendrocytes. Moreover, the detection of MeCP2 in glia, including astrocytes, oligodendrocytes and microglia, signifies that an accurate level of MeCP2 in glia is critical to the normal development to of glia and neurons in the vicinity (Ballas et al., 2009; Lioy et al., 2011; Maezawa et al., 2009; Nguyen et al., 2013; Sharma et al., 2015). Therefore, the precise level of MeCP2 and its phosphorylation is important during OLG development.

Till date, it has been believed that MeCP2 is a nuclear protein (Cohen et al., 2011; Gonzales et al., 2012; Mnatzakanian et al., 2004) although a previous report showing that MeCP2 can be localized from the cytoplasm to the nucleus upon neuronal differentiation by dephosphorylation on serine sites. Moreover, the findings suggest that phosphorylation controls the transcriptional function of MeCP2 by regulating its intracellular localization (Miyake and Nagai, 2007). A recent study showed in rat brain there is nuclear localization of MeCP2 and pS80MeCP2 while pS421MeCP2 and pS292MeCP2 were mainly expressed in the cytoplasmic compartment (Liu et al., 2017).

In agreement with this finding, it was found that pS421 MeCP2 is mainly localized in the cytoplasm, whereas MeCP2 and pS80 MeCP2 was found in the nucleus of astrocytes and C6 glioma cells (Figs. 3.8, 3.9 and 3.10). These findings are consistent with published reports showing that MeCP2 localize outside the nucleus (Mnatzakanian et al., 2004) and in the post-synaptic compartment (Aber et al., 2003). Nevertheless, one study has shown that MeCP2 is detectable in the cytoplasm of undifferentiated PC12 cells in a phosphorylated form (Miyake and Nagai, 2007). MeCP2 deficiency in astrocytes impacts the expression of glial intermediate filament proteins such as fibrillary acidic protein (GFAP) and S100 and induces neuron toxicity by disturbing glutamate metabolism or enhancing microtubule instability (Forbes-Lorman et al., 2014).

Chapter-3

To study the expression and sub-cellular localization of MeCP2 in glial cells

MeCP2 positively as well as negatively modulates the gene transcription (Bellini et al.; Chao and Zoghbi, 2009; Cheng et al., 2014; Rutlin and Nelson, 2011). Studies have shown that phosphorylation of MeCP2 is the key mechanism by which MeCP2 binds at specific promoters by modulating the affinity for it partners thereby leading to differential gene expression (Jung et al., 2003; Li et al., 2011;Tao et al., 2009). pS80& pS421MeCP2 phosphorylation are primarily expressed in neurons, however recent insights have also demonstrated its expression in astrocytes (Liu et al., 2017). MeCP2 although detectable in glial cells at significantly lower levels, is very critical in proper development of neurons (Lioy et al., 2011; Maezawa et al., 2009; Nguyen et al., 2013).

Taken together, our data provide the first evidence that the patterns of expression and distribution of MeCP2 and diverse pMeCP2s are distinct and vary with the glial cell development. Moreover, MeCP2 and pS80 MeCP2 are concentrated in the nucleus, while pS421 MeCP2 are mainly localized in the cytoplasm. Furthermore, MeCP2 and the pMeCP2s are predominantly expressed in neurons, but are also detectable in astrocytes, oligodendrocytes and C6 glioma cell line at a relatively low level. Until now, the patterns of expression of pMeCP2s remain unclear. The results from the present study suggest that MeCP2 phosphorylation distribution and expression pattern differ from cell to cell.

Recent studies have shown that MeCP2 phosphorylation is stimuli dependent and it is regulated by several developmental growth factors (Li and Chang 2014). It would be very interesting to see how some of the growth factors can modulate the MeCP2 phosphorylation and its localization. Hence, we hypothesized that "MeCP2 in glial cells is regulated by stimuli mediated phosphorylation which would allow MeCP2 to bind to distinct sites with an effect on chromatin affinity through sub-cellular localization", which is discussed in detail in the chapters 4 and 5.

Fig.3.1 (A)

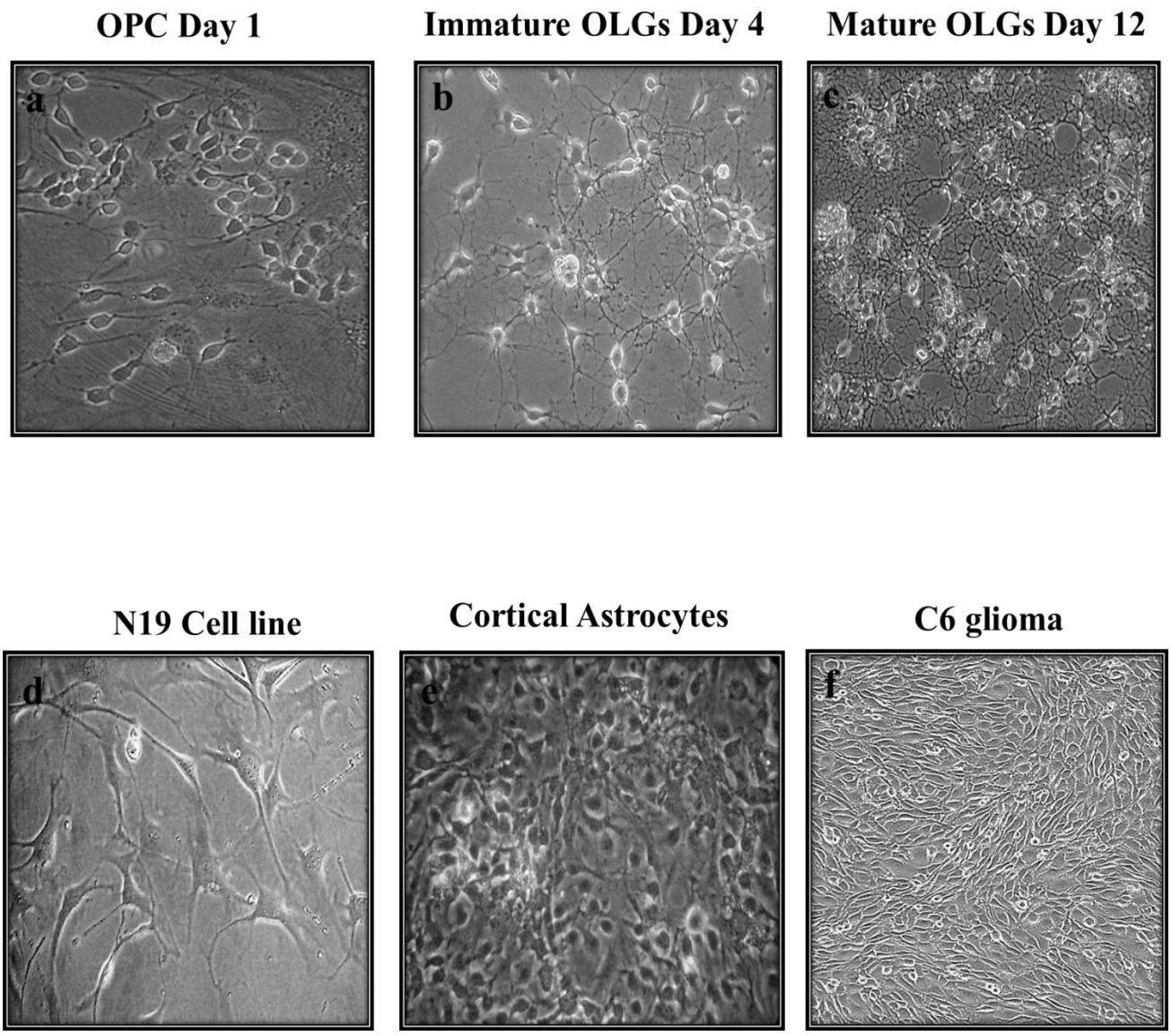
OPC Day 1
Immature OLGs Day 4
Mature OLGs Day 12
a
b
c
N19 Cell line
Cortical Astrocytes
C6 glioma
d
e
f

Fig. 3.1 (B)

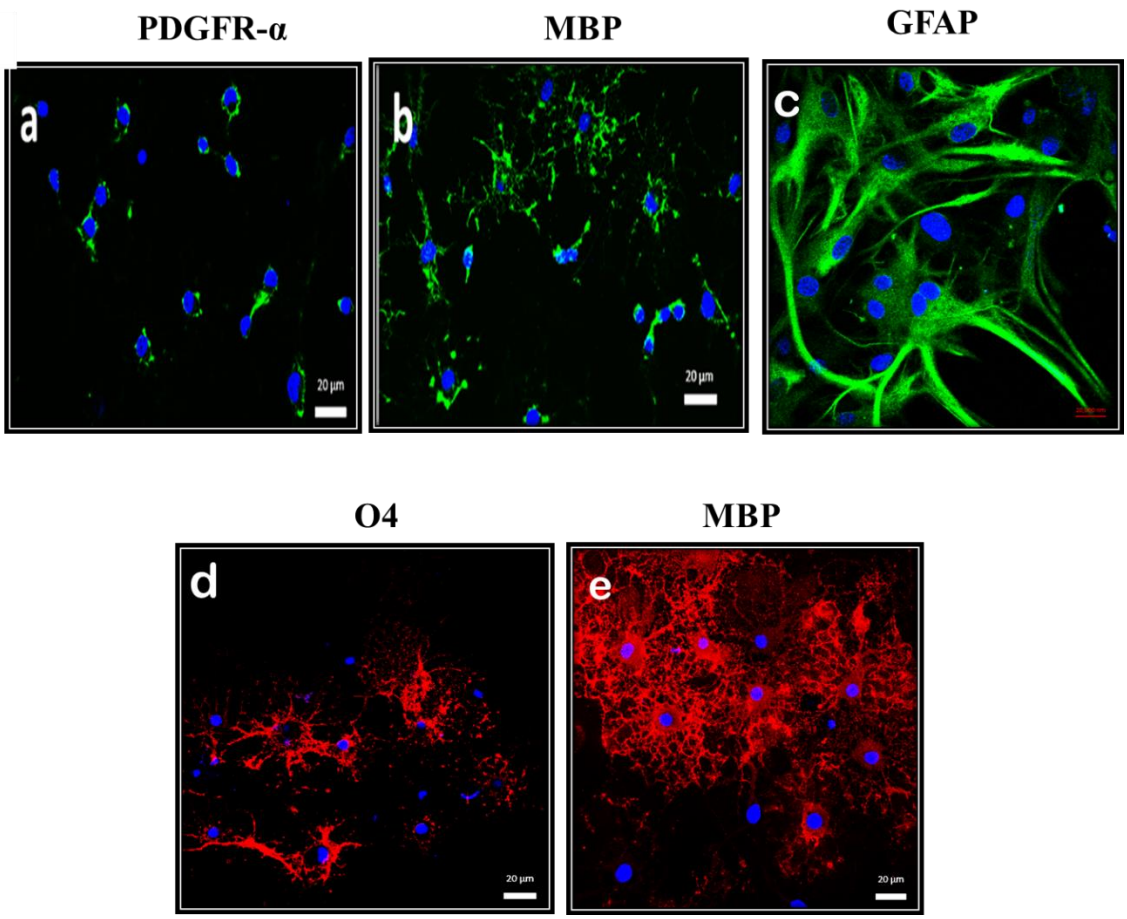

Fig. 3.1 Characterization of glial cells (A)- *Phase contrast images and Morphological characterization of isolated glial cells: (a) Oligodendrocyte progenitor cells (OPCs) Day-1 were plated and allowed to grow in B27 media containing PDGF-A (proliferation medium), After 24hrs post plating, cultures were entirely switched to Sato media without PDGF-A (differentiation medium) and analyzed. (b) Immature OLGs; Day-4, (c) Mature OLGS; Day-12, (d) N19 cell line, (e) Cortical Astrocytes after shake, (f) C6 glioma cell line* ***(B)*** *Characterization of glial cells with cell specific markers. Representative Immunostaining images showing (a)- Immature N19 characterized with anti-PDGFRα (green), (b) Mature N19 with anti-MBP (green), (c) Cortical astrocytes with anti-GFAP (green), After overnight shaking, isolated oligodendrocytes were fixed, followed by Immunostaining, (d) Immature OLGs with anti-O4(red) at Day-4, (e) Mature OLGs with anti-MBP(red Day-12, The nucleus was stained with 4',6-diamidino-2-phenylindole- DAPI (blue). Scale bar=20µm (DAPI).*

Fig. 3.2 (A)

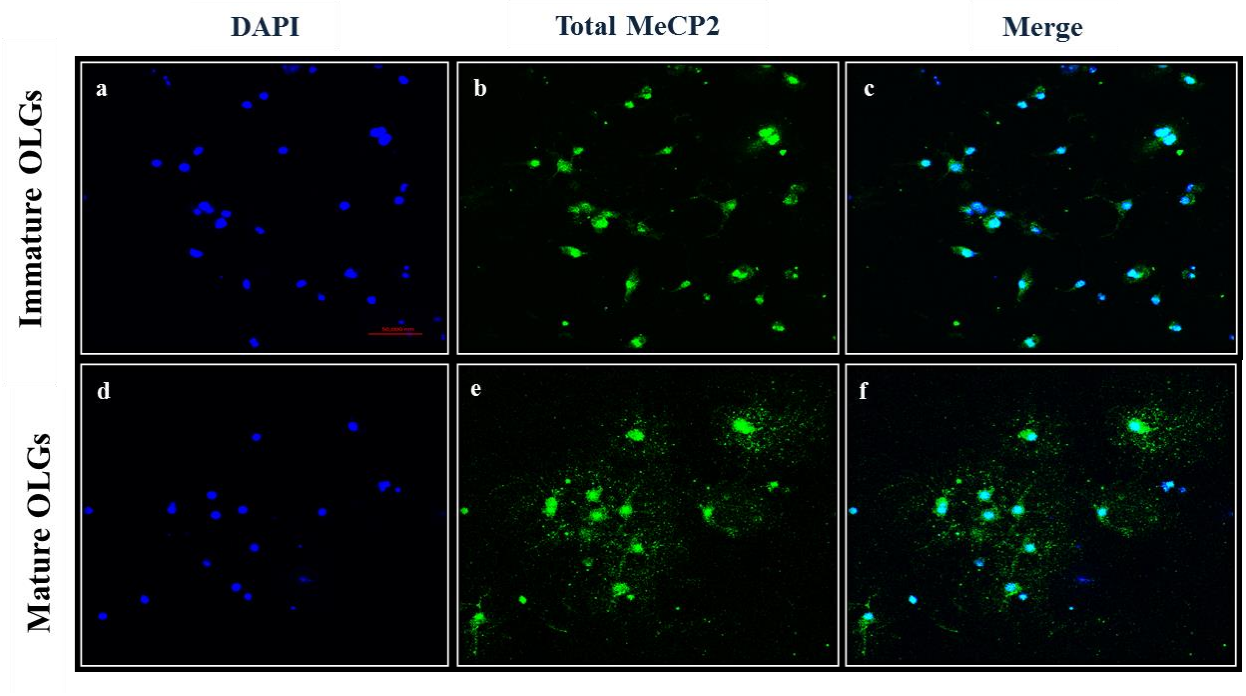

Fig.3.2 (B)

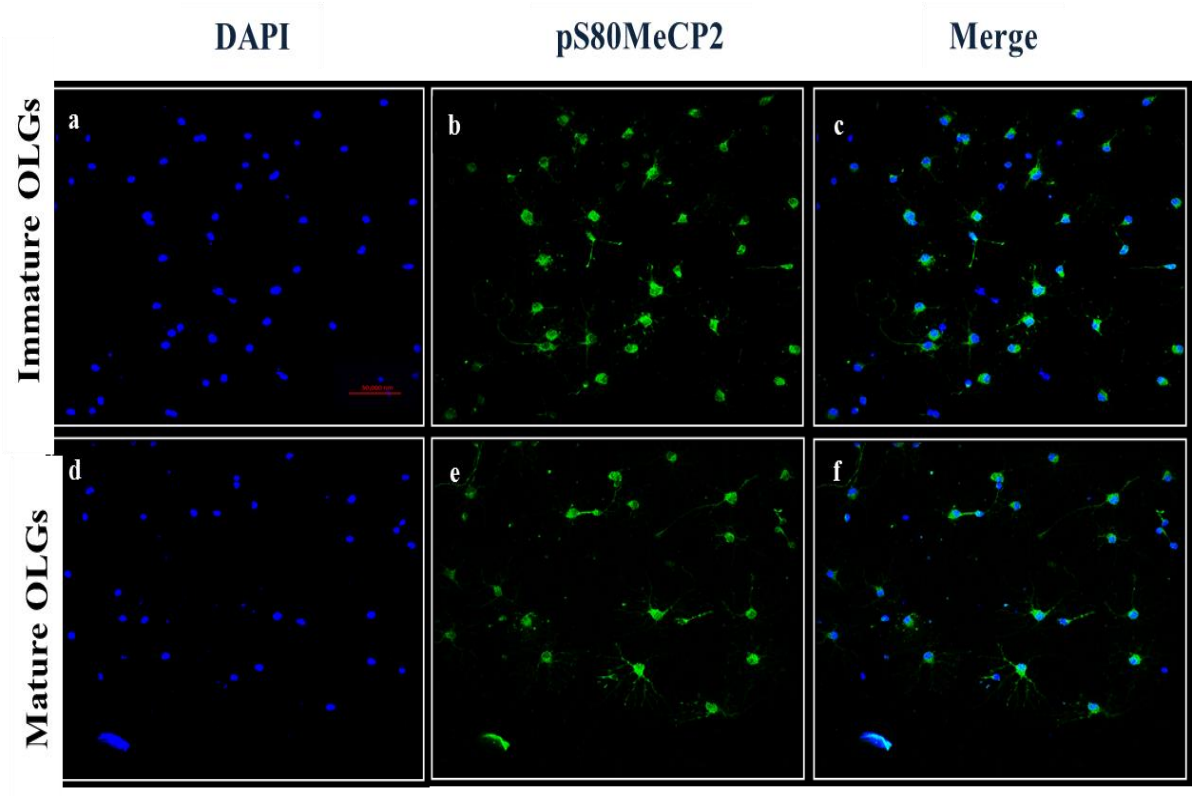

Fig.3.2

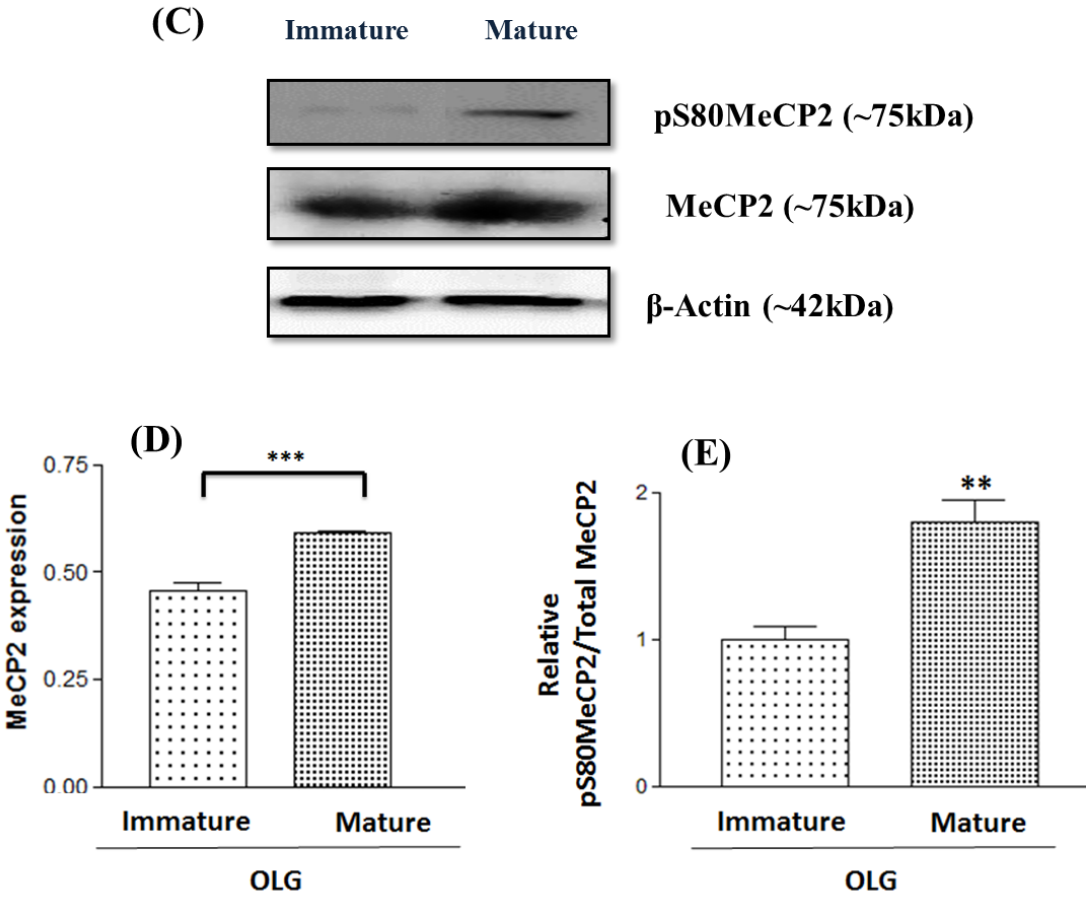

Fig.3.2 MeCP2 expression in oligodendroglial cells. ***(A)*** *Representative Immunostaining images showing MeCP2 and* ***(B)*** *pS80MeCP2 expression in immature and mature oligodendroglial cells (green). The nucleus was stained with DAPI (blue). Scale bar=50µm.* ***(C)*** *Representative Western blot for phosphorylated and total MeCP2 in lysates of immature and mature oligodendroglial cells showing increased expression of in mature OLGs compared to immature OLGs.* ***(D)*** *After densitometric analysis, MeCP2 was normalized to β-Actin and represented in graphical form.****(E)*** *After densitometric analysis pS80MeCP2 data was normalized to total MeCP2and represented in graphical form. Three different cell preparations were analyzed three times N= 3. Error bars represent ± SEM. Data were evaluated using student's t test or One way ANOVA -parameter where appropriate (*P<0.05, **P<0.01, ***P<0.001).*

Fig.3.3

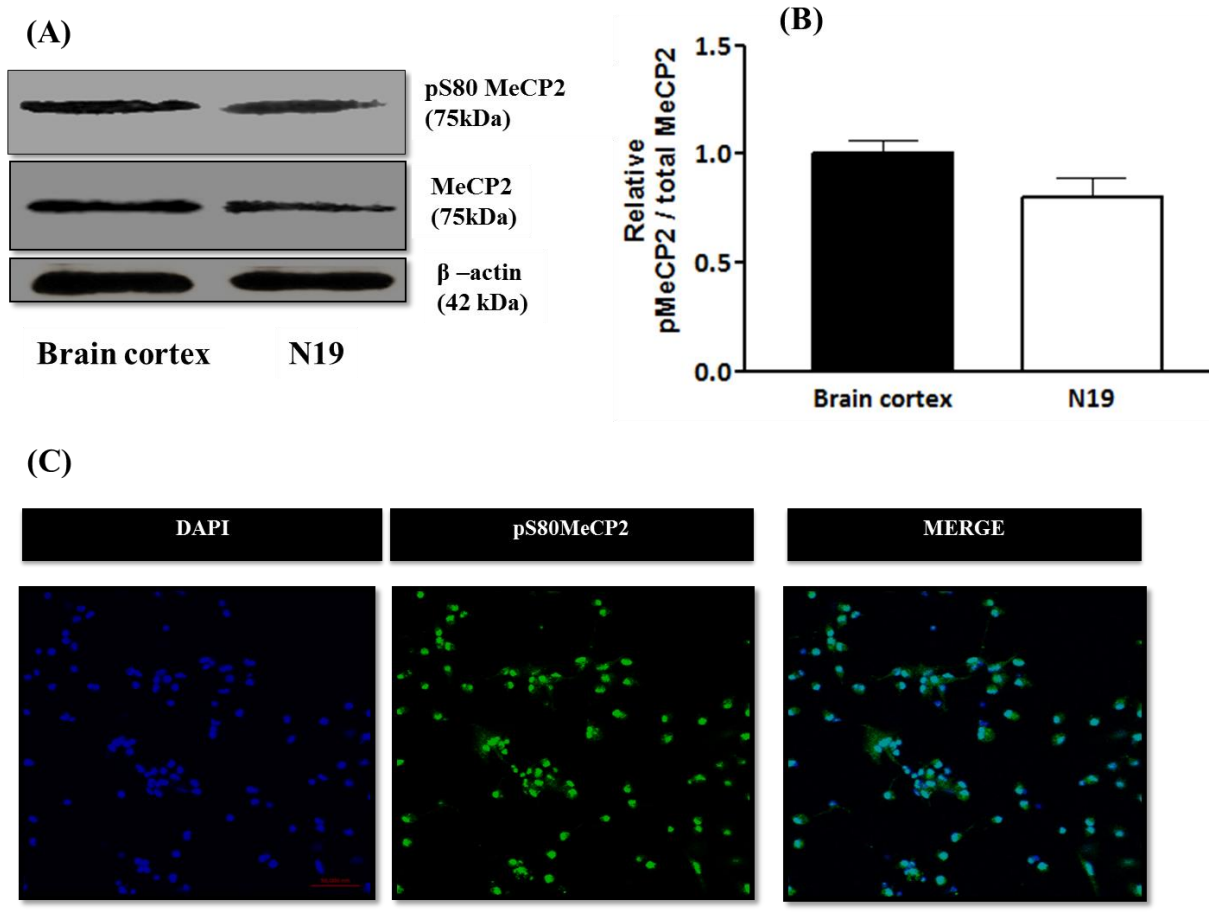

Fig.3.3 pS80MeCP2 expression and distribution in N19 oligodendroglial cells. (A) *Representative Western blot for phosphorylated and total MeCP2 in lysates of brain cortex and N19 oligodendroglial cells.* ***(B)*** *After densitometric analysis, pS80MeCP2 data were normalized to total MeCP2. Three different cell preparations were analyzed three times N= 3. Error bars represent ± SEM.* ***(C)*** *Representative Immunostaining images showing pS80MeCP2 expression in N19 oligodendroglial cells (green). The nucleus was stained with DAPI (blue). Scale bar=50µm. Data were evaluated using student's t test or One way ANOVA -parameter where appropriate (*P<0.05, **P<0.01, ***P<0.001).*

Fig. 3.4

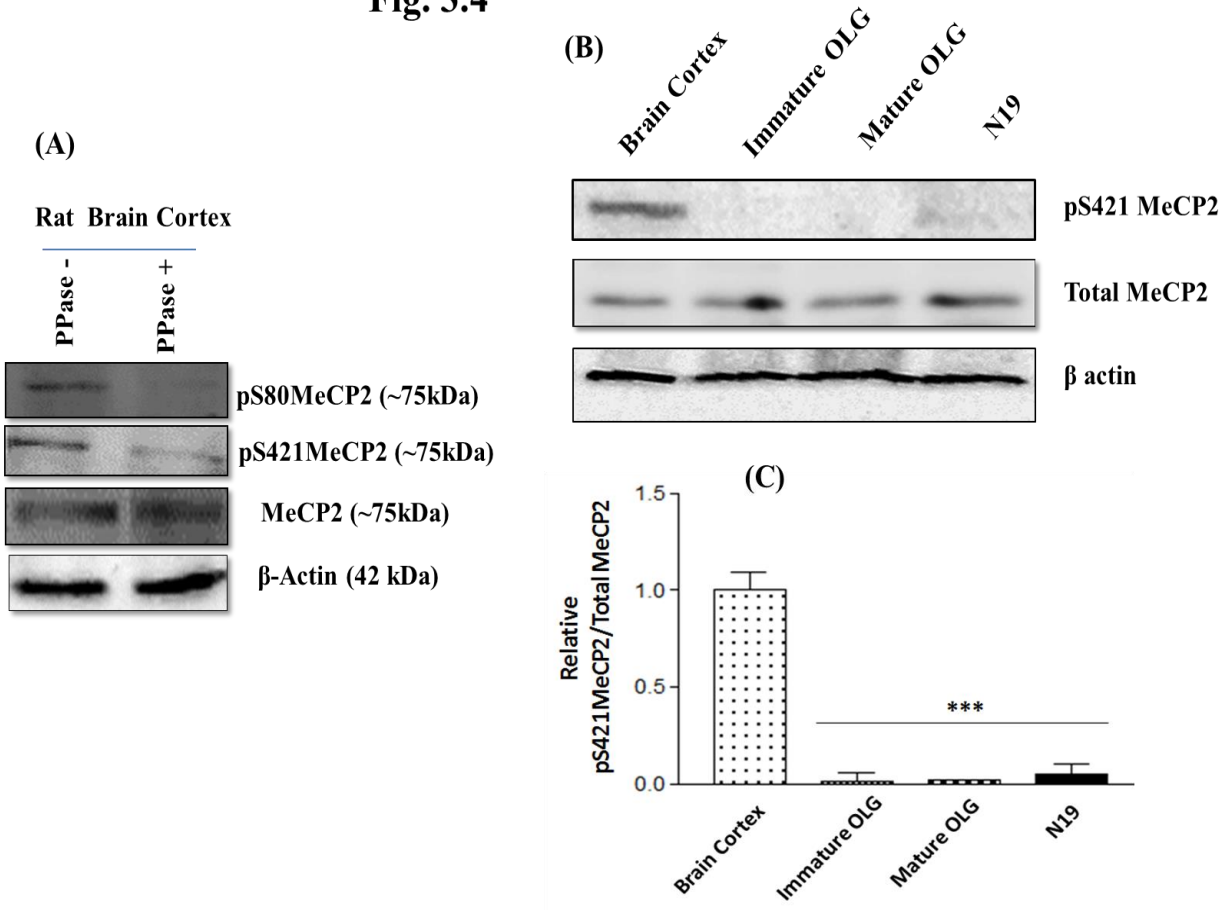

Fig. 3.4 Expression of pS421MeCP2 in oligodendrocytes: *(A)Representative western Blots for pS80MeCP2 and pS42MeCP2 from rat brain cortex and the bands were abolished upon alkaline phosphatase treatment. (B)Representative Western blot for pS421MeCP2 and MeCP2 in lysates of brain cortex, immature and mature OLGs and N19 OLGs. (C)Graph shows no expression of pS421 MeCP2 in OLGs. Three different cell preparations were analyzed three times N= 3. Values represent mean ± SEM. Statistical differences between the stimulated and control samples were determined using Student's t test or one-way ANOVA parameter where appropriate (*P < 0.05, **P < 0.01, ***P < 0.001).*

Fig. 3.5

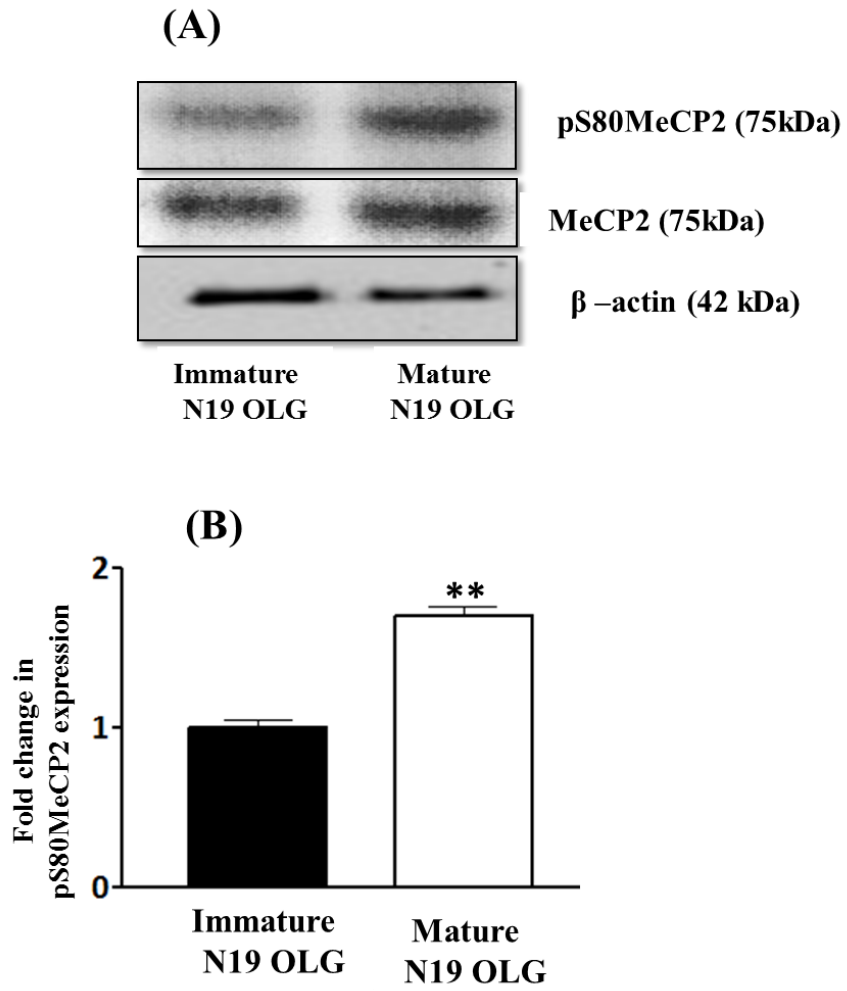

Fig.3.5 pS80MeCP2 expression in immature and mature N19 OLGs: *(A)Representative Western blots for pS80MeCP2 in immature and mature N19 OLGs. (B)Graph shows increased levels of pS80MeCP2 in mature N19 OLGs. Three different cell preparations were analyzed three times N= 3. Values represent mean ± SEM. Statistical differences between the stimulated and control samples were determined using Student's t test or one-way ANOVA parameter where appropriate (*P < 0.05, **P < 0.01, ***P < 0.001).*

Fig 3.6

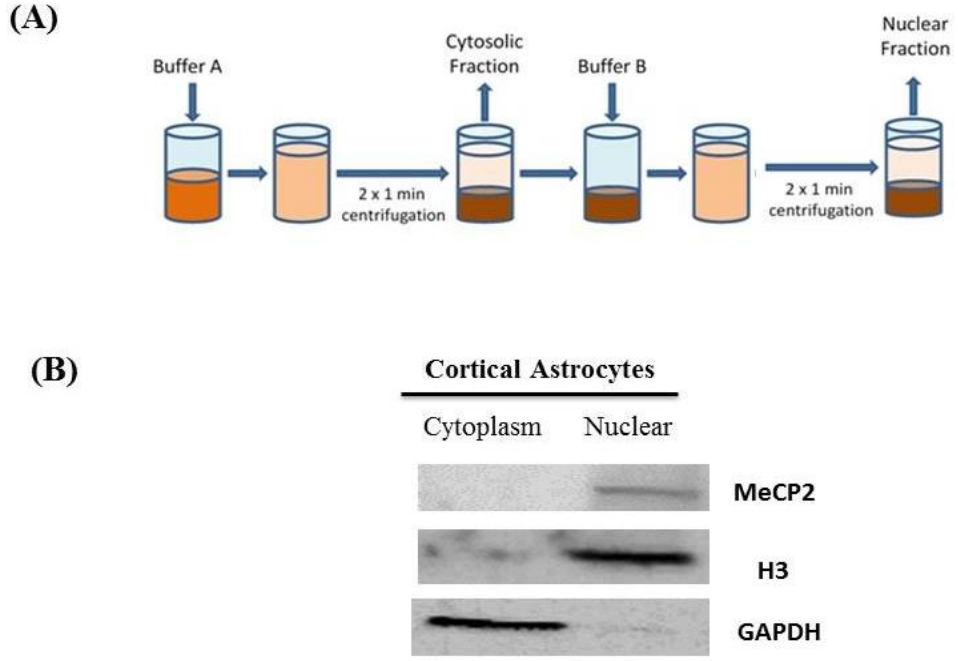

Fig.3.6 Optimization of Cytoplasmic and Nuclear extraction*: (A) Diagrammatic representation of the cell fraction preparation. (B)Western blot analysis was applied to the cytoplasmic and nuclear proteins isolated from cortical astrocytes. MeCP2 was mainly found in the nuclear fraction. GAPDH was used as loading controls for the cytoplasmic proteins, and H3 for the nuclear proteins.*

Fig 3.7 (A)

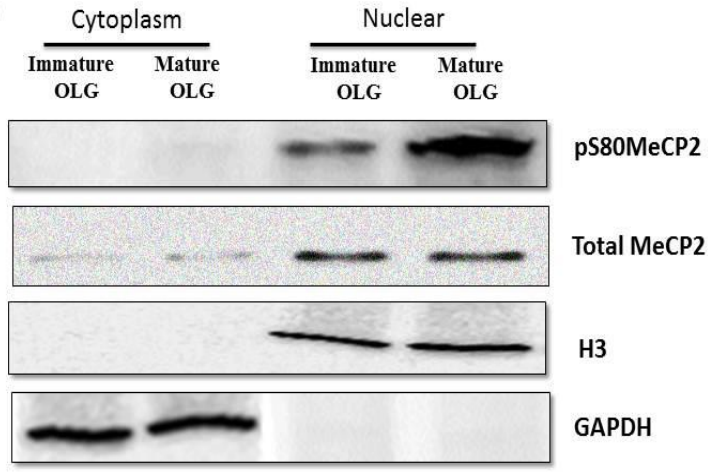

(B)

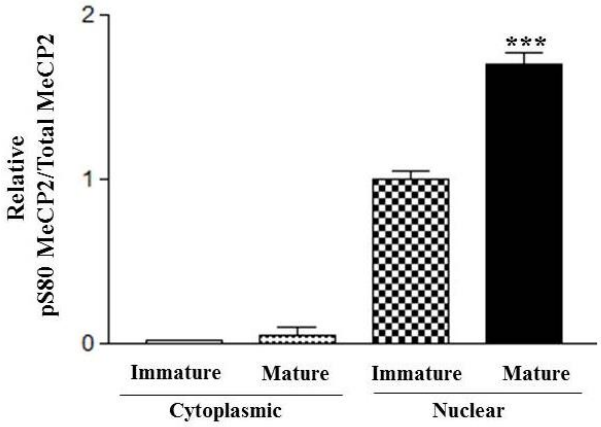

Fig. 3.7 Expression and intracellular localization of MeCP2 and the pMeCP2s in OLGs*: (A) Western blot analysis was applied to the cytoplasmic and nuclear proteins. MeCP2 and pS80MeCP2 were mainly found in the nuclear fraction. GAPDH was used as internal control for the cytoplasmic proteins, and H3 for the nuclear proteins.(B) After densitometric analysis, pS80MeCP2 and MeCP2 data were normalized to the loading controls of cytoplasmic and nuclear fractions. Three different cell preparations were analyzed three times N= 3. Values represent mean ± SEM. Statistical differences between the stimulated and control samples were determined using Student's t test or one-way ANOVA parameter where appropriate (*P < 0.05, **P < 0.01, ***P < 0.001).*

Fig. 3.8

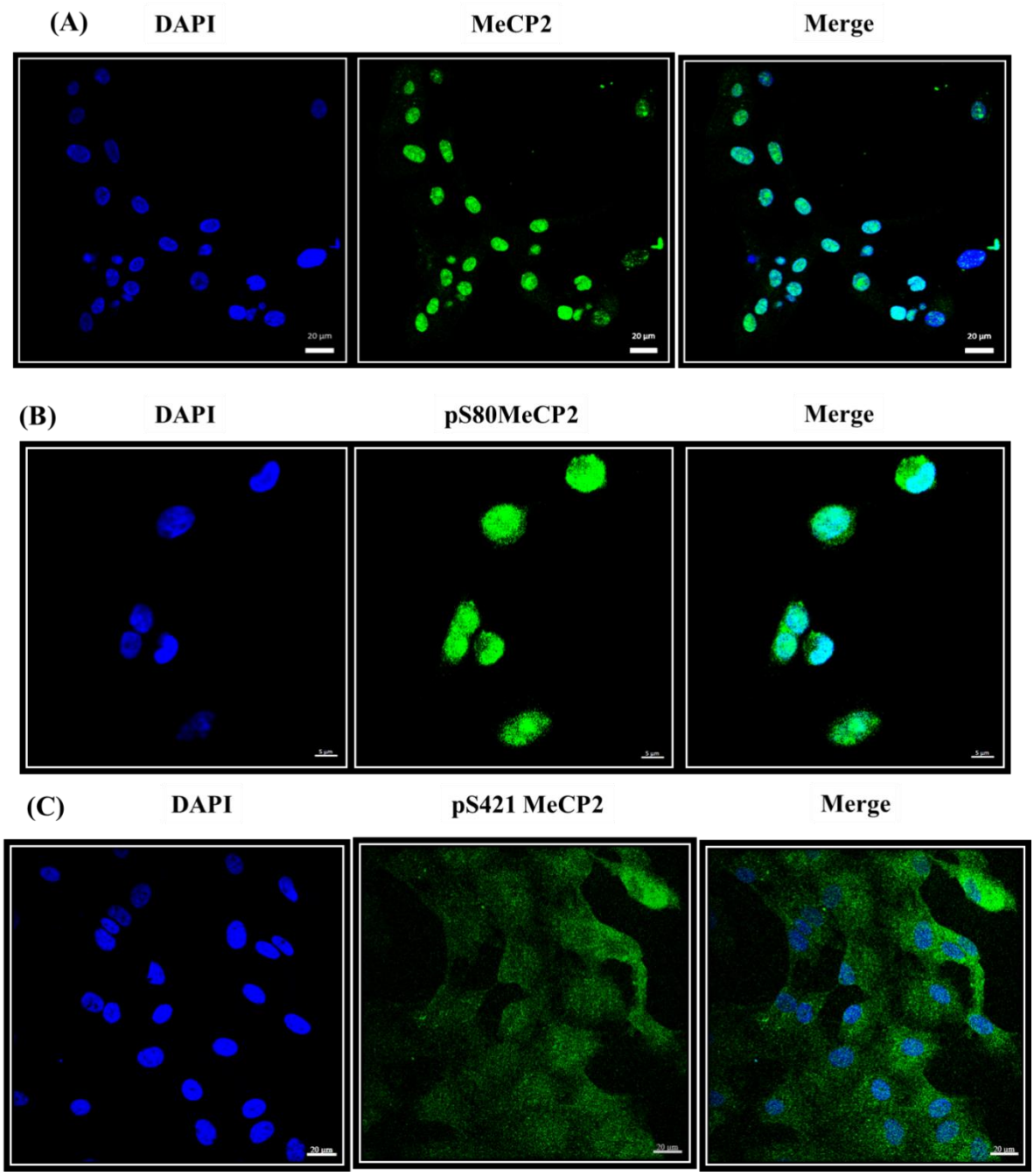

Fig.3.8 Intracellular localization of MeCP2 and the pMeCP2s in the postnatal rat cortical astrocytes *Confocal images of immunofluorescent double staining of MeCP2, pS80MeCP2 &pS421MeCP2, (green) with DAPI (blue) in the cortical astrocytes. MeCP2 (A) and pS80MeCP2 (B) were colocalized with DAPI, whereas pS421 MeCP2 (C) were mostly excluded from and enwrapped the DAPI-labeled nucleus. Scale bars 20µm (A & C) and 5µm (B)*

Fig. 3.9

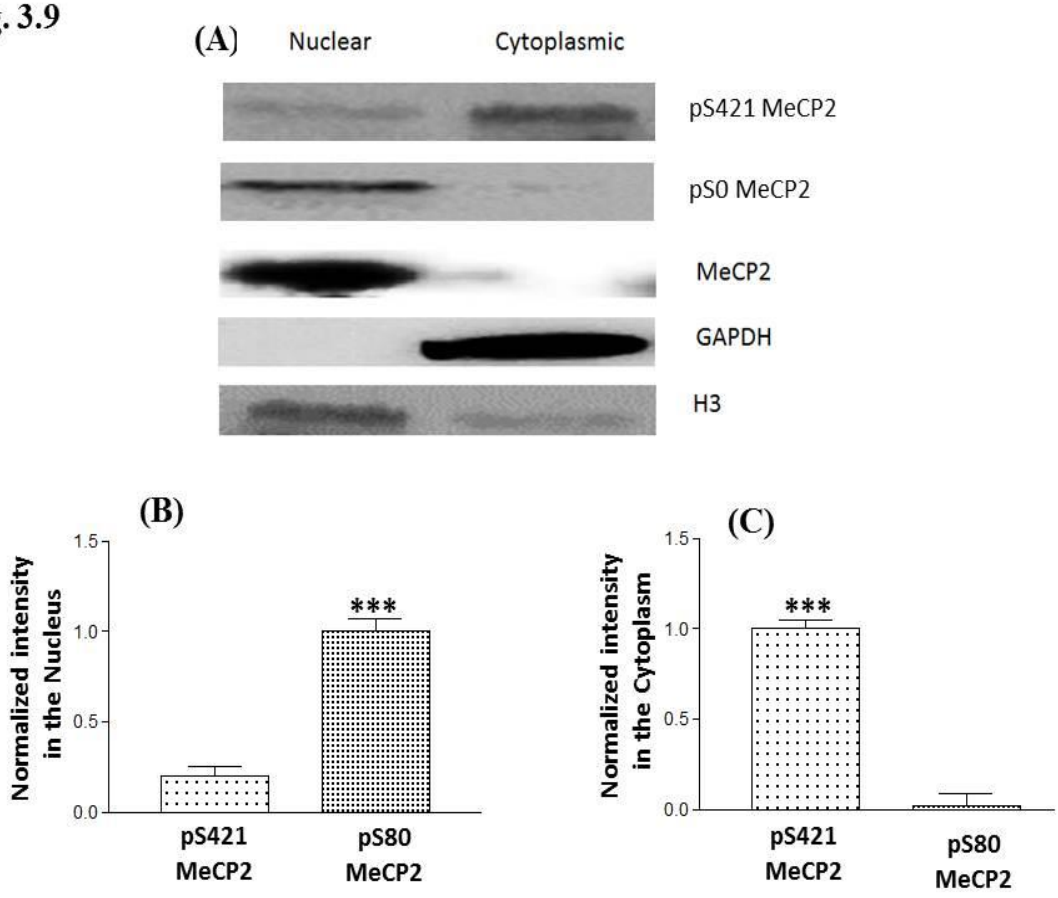

Fig. 3.9 Expression and intracellular localization of MeCP2 and the pMeCP2s in the cortical astrocytes: *(A) Western blot analysis was applied to the cytoplasmic and nuclear proteins. MeCP2 and pS80 MeCP2 were mainly found in the nuclear fraction, while pS421 MeCP2 was more concentrated in cytoplasm than nucleus. GAPDH was used as internal control for the cytoplasmic proteins, and H3 for the nuclear proteins.(B) After densitometric analysis, pS80MeCP2 an pS421MeCP2 data were normalized to the loading controls of cytoplasmic and nuclear fractions. Three different cell preparations were analyzed three times N= 3. Values represent mean ± SEM. Statistical differences between the stimulated and control samples were determined using Student's t test or one-way ANOVA parameter where appropriate(*P < 0.05, **P < 0.01, ***P < 0.001).*

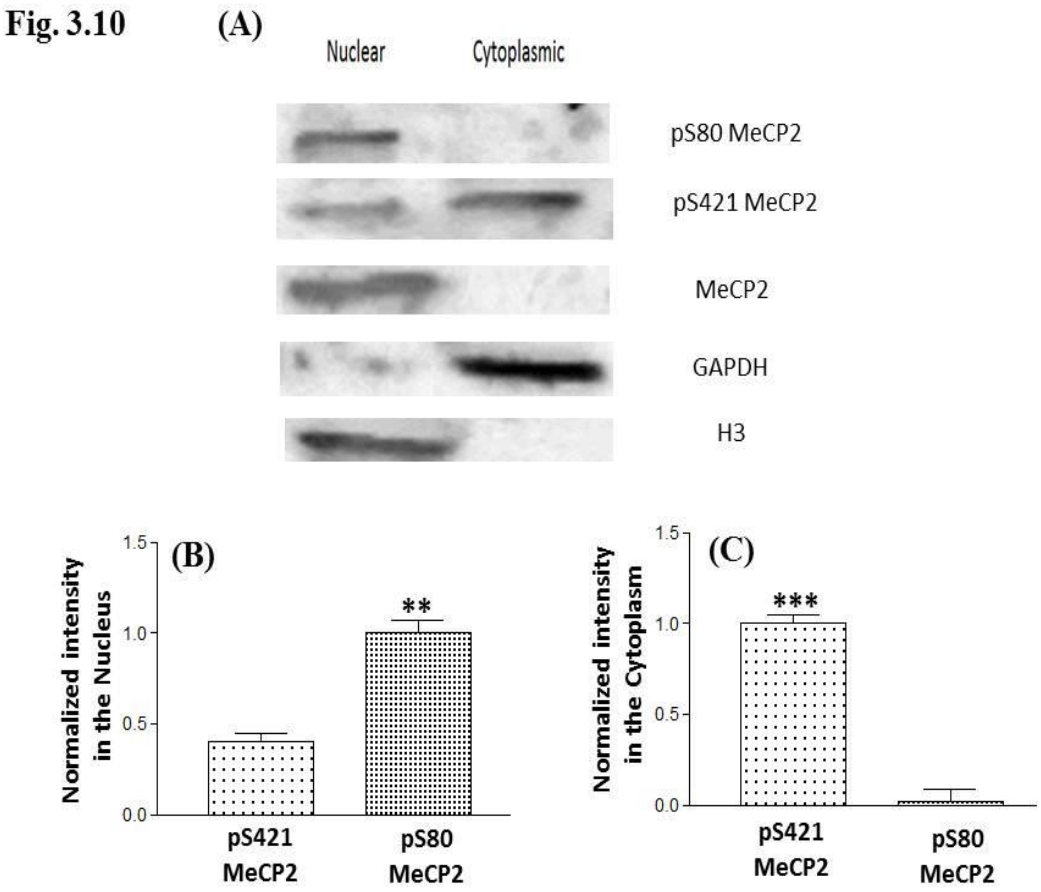

Fig. 3.10 Expression and intracellular localization of MeCP2 and the pMeCP2s in the C6 glioma: *(A) Western blot analysis was applied to the cytoplasmic and nuclear proteins. MeCP2 and pS80MeCP2 were mainly found in the nuclear fraction, while pS421MeCP2 was more concentrated in cytoplasm than nucleus. GAPDH was used as controls for the cytoplasmic proteins, and H3 for the nuclear proteins.(B) After densitometric analysis, pS80MeCP2 an pS421MeCP2 data were normalized to the loading controls of cytoplasmic and nuclear fractions. Three different cell preparations were analyzed three times N= 3. Values represent mean ± SEM. Statistical differences between the stimulated and control samples were determined using Student's t test or one-way ANOVA parameter where appropriate(*P < 0.05, **P < 0.01, ***P < 0.001).*

Fig. 3.11

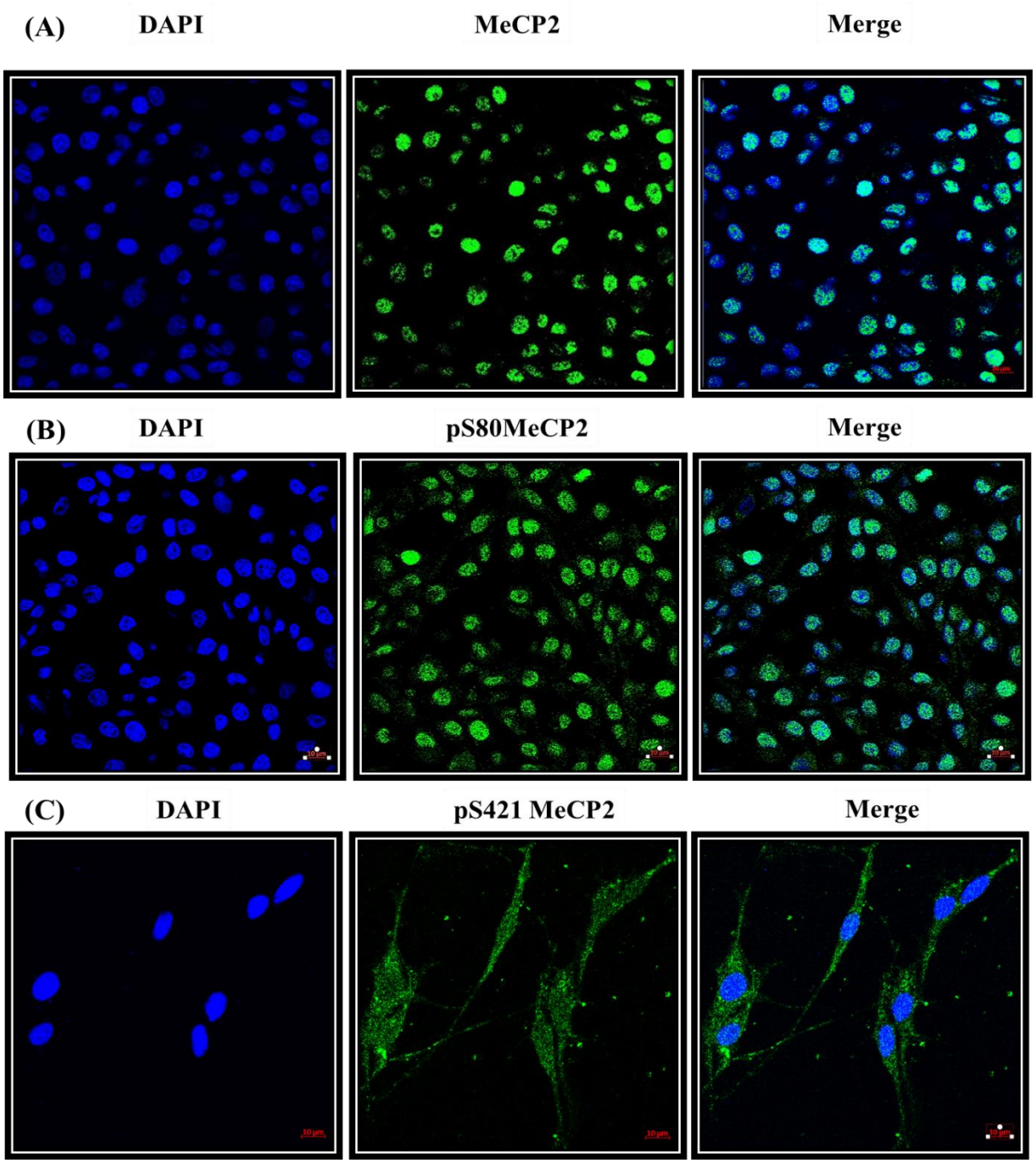

Fig. 3.11 Intracellular localization of MeCP2 and the pMeCP2s in the C6 glioma cell line: *Confocal images of immunofluorescent double staining of MeCP2, pS80MeCP2, pS421MeCP2, (green) with DAPI (blue) in the cortical astrocytes. MeCP2 (A) and pS80MeCP2 (B) were colocalized with DAPI, whereas pS421MeCP2 (C) were mostly excluded from and enwrapped the DAPI-labeled nucleus. Scale bars 10µm*